# Time lags and reverberation in the lamp-post geometry of the compact corona illuminating a black-hole accretion disc

Michal Dovčiak

Astronomical Institute
Academy of Sciences of the Czech Republic, Prague

*Astrophysics group seminar, Department of Physics, University of Crete, Heraklion, Greece*

30$^{th}$ May 2014

# Acknowledgement

**StrongGravity** (2013–1017) — EU research project funded under the Space theme of the 7th Framework Programme on Cooperation

Title: **Probing Strong Gravity by Black Holes Across the Range of Masses**

Institutes: AsU, CNRS, UNIROMA3, UCAM, CSIC, UCO, CAMK

Webpages: `http://stronggravity.eu/`

`http://cordis.europa.eu/projects/rcn/106556_en.html`



# Active Galactic Nuclei – scheme

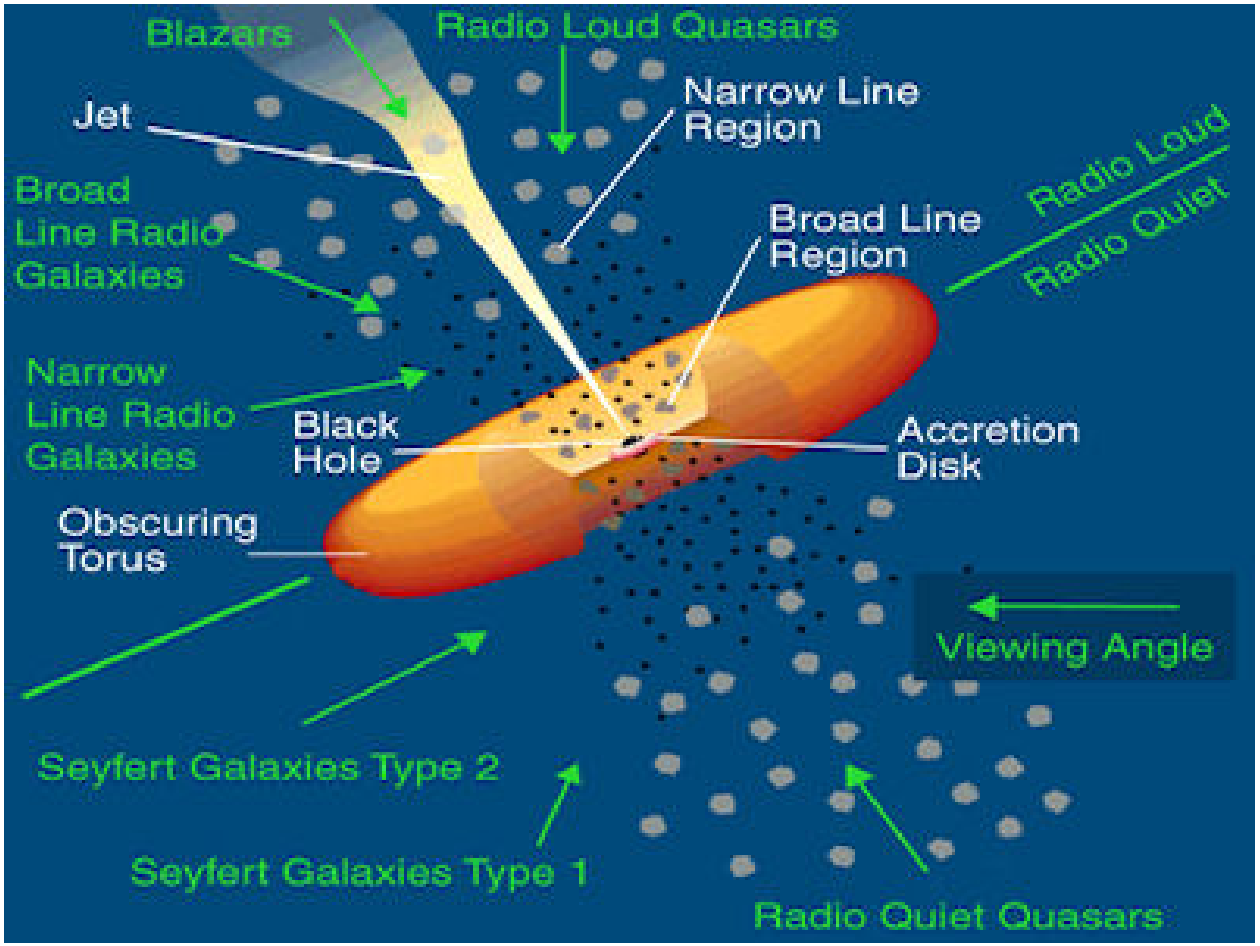


Urry C. M. & Padovani P. (1995)
*Unified Schemes for Radio-Loud Active Galactic Nuclei*
PASP, 107, 803

# Active Galactic Nuclei – X-ray spectrum

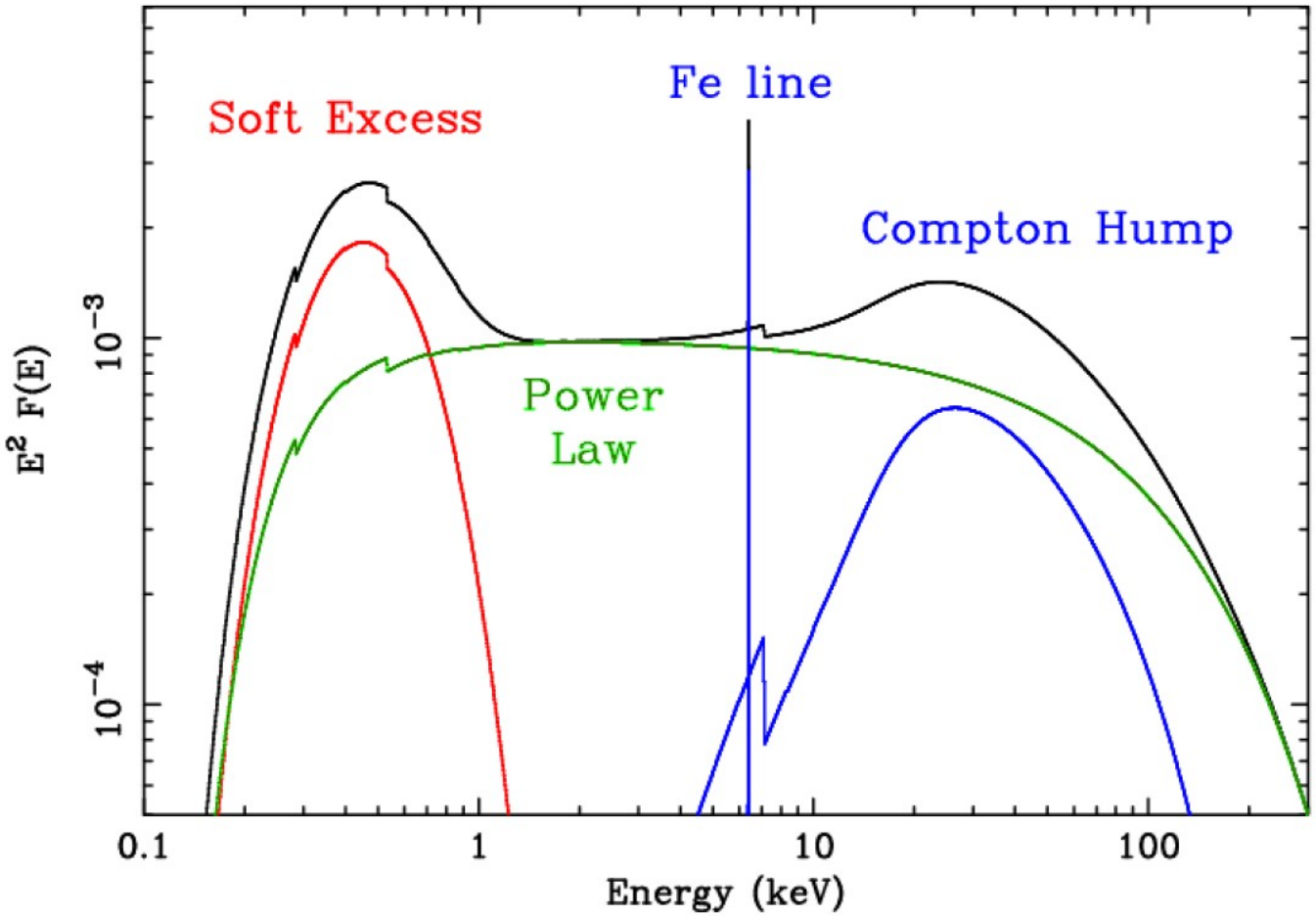


Fabian A.C. (2005)
*X-ray Reflections on AGN*,
in proceedings of "The X-ray Universe 2005", El Escorial, Madrid, Spain, 26-30/9/2005

# Active Galactic Nuclei – lags

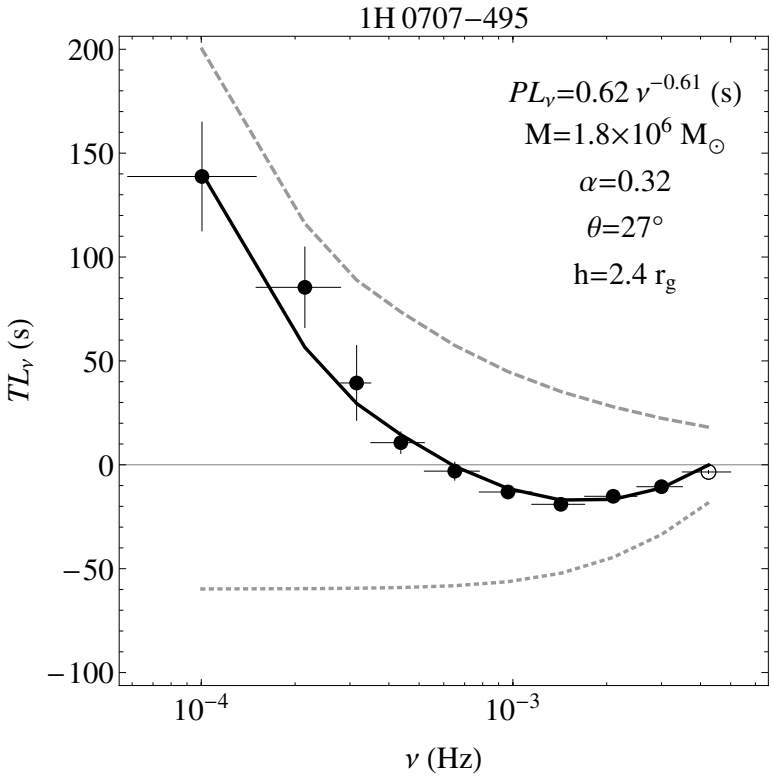


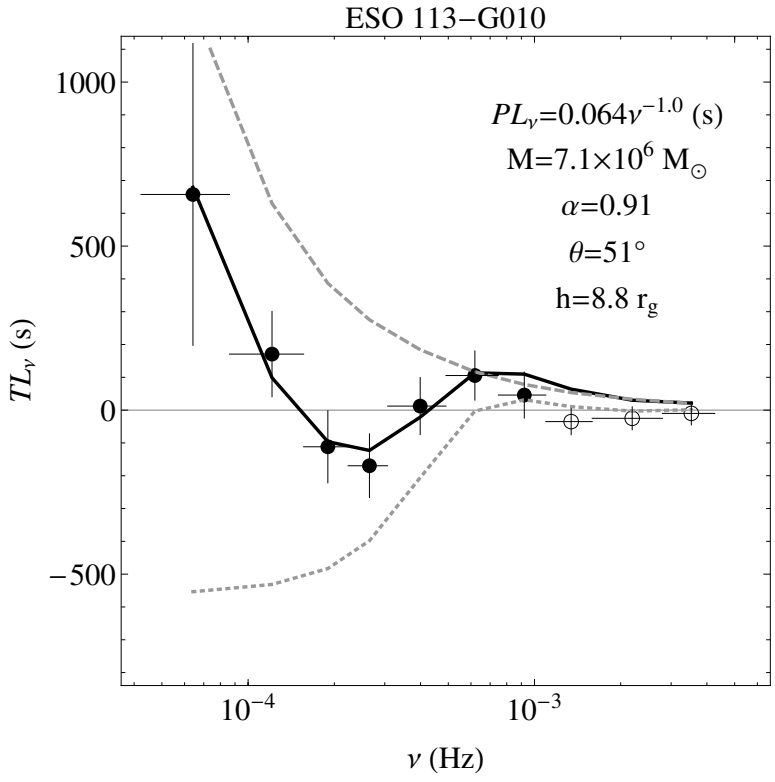


Emmanoulopoulos et al. (2014)
*General relativistic modelling of the negative reverberation X-ray time delays in AGN*, MNRAS **439** 3931

# Active Galactic Nuclei – lags

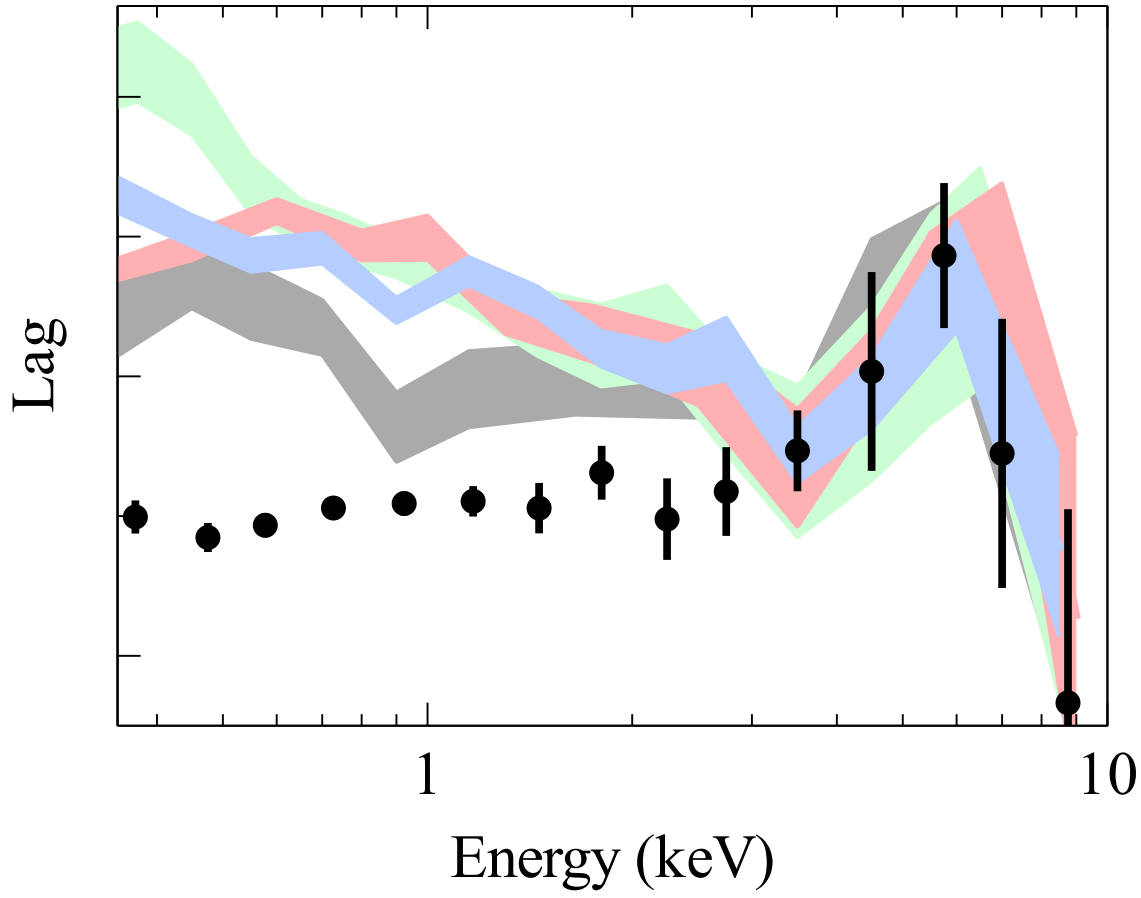


Kara et al. (2014)
*The curious time lags of PG 1244+026: Discovery of the iron K reverberation lag*, MNRAS **439** L26

# References

- Blandford & McKee (1982) ApJ **255** 419 $\rightarrow$ reverberation of BLR

$$L_{\rm o}(v,t) = \int_{-\infty}^{\infty} dt'\, L_{\rm p}(t')\, \Psi(v, t-t')$$

- Stella (1990) Nature **344** 747 $\rightarrow$ time dependent Fe K$\alpha$ shape ($a = 0$)
- Matt & Perola (1992) MNRAS **259** 433
  $\rightarrow$ Fe K$\alpha$ response and black hole mass estimate $\rightarrow t \sim GM/c^3$
  $\rightarrow$ time dependent light curve, centroid energy and line equivalent width ($h = 6, 10$; $a = 0$; $\theta_{\rm o}$)
- Campana & Stella (1995) MNRAS **272** 585
  $\rightarrow$ line reverberation for a compact and extended source ($a = 0$)
- Reynolds, Young, Begelman & Fabian (1999) ApJ **514** 164
  $\rightarrow$ fully relativistic line reverberation ($h = 10$; $a = 0, 1$)
  $\rightarrow$ more detailed reprocessing, off-axis flares
  $\rightarrow$ ionized lines for Schwarzschild case, outward and inward echo, reappearance of the broad relativistic line

# References

More recent references:


- Chainakun & Young (2012) MNRAS **420** 1145
  $\rightarrow$ fully relativistic, lamp-post geometry, ionized accretion disc
- Wilkins & Fabian (2013) MNRAS **430** 247
  $\rightarrow$ fully relativistic, extended corona, propagation effects
- Cackett et al. (2014) MNRAS **438** 2980
  $\rightarrow$ Fe K$\alpha$ reverberation in lamp-post model (spectral line)
- Emmanoulopoulos et al. (2014) MNRAS **439** 3931
  $\rightarrow$ Fe K$\alpha$ reverberation in lamp-post model (soft excess)

# Why to study toy model of lamp-post geometry?

- physical motivation: base of a jet
- many effects should be qualitatively similar with this simple geometry
- it can give us certain limits on the model (e.g. spin versus height)
- we can easily explore the dependence on many parameters (height of the corona, ionization of the disc, ...)
- if we want to study the dependence on geometry, we should know how other parameters influence the results

  (i.e. *Is the idea of measuring geometry of the corona via reverberation feasible?*)

# Scheme of the lamp-post geometry

- central black hole – mass, spin
- compact corona with isotropic emission
  → height, photon index
- accretion disc
  → Keplerian, geometrically thin, optically thick
  → ionisation due to illumination
  ($L_p$, $h$, $M$, $a$, $n_H$, $q_n$)
- local re-processing in the disc
  → REFLIONX with different directional emissivity prescriptions
- relativistic effects:
  → Doppler and gravitational energy shift
  → light bending (lensing)
  → aberration (beaming)
  → light travel time

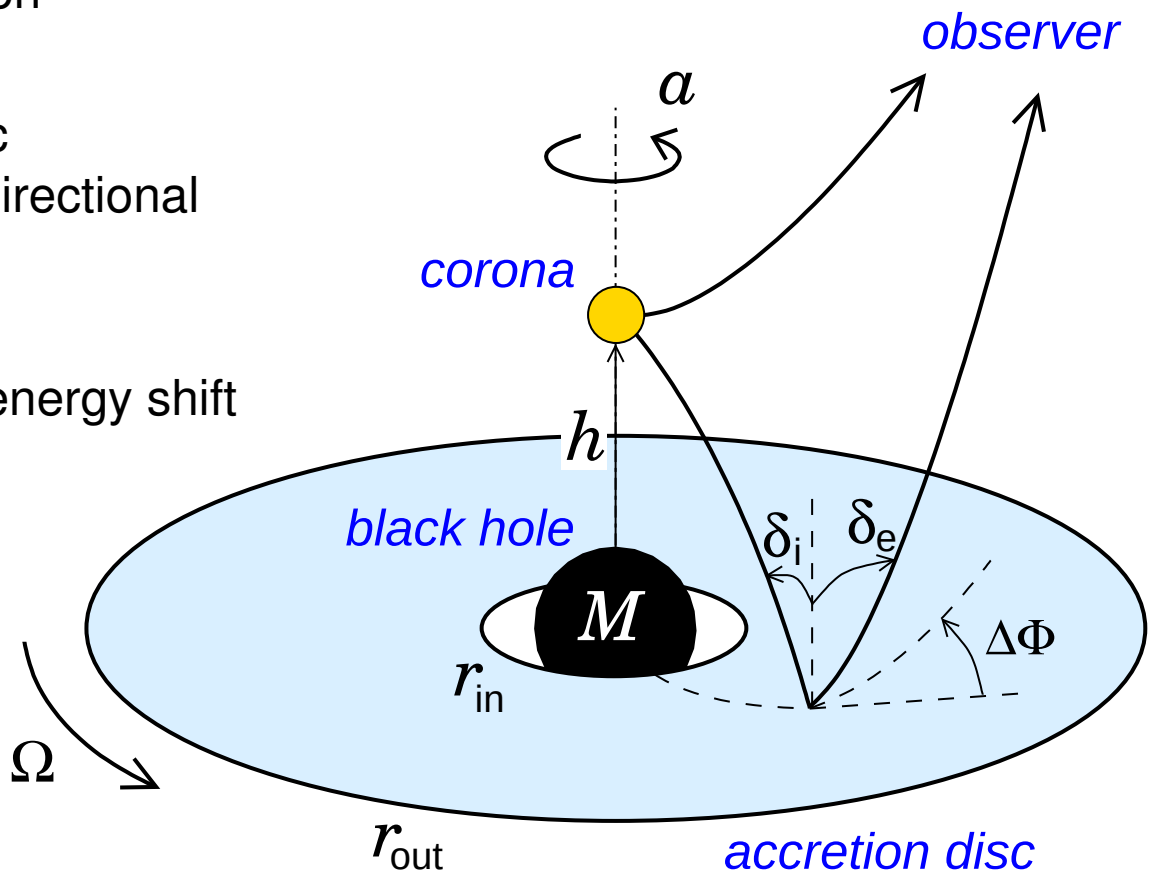

# Time delay

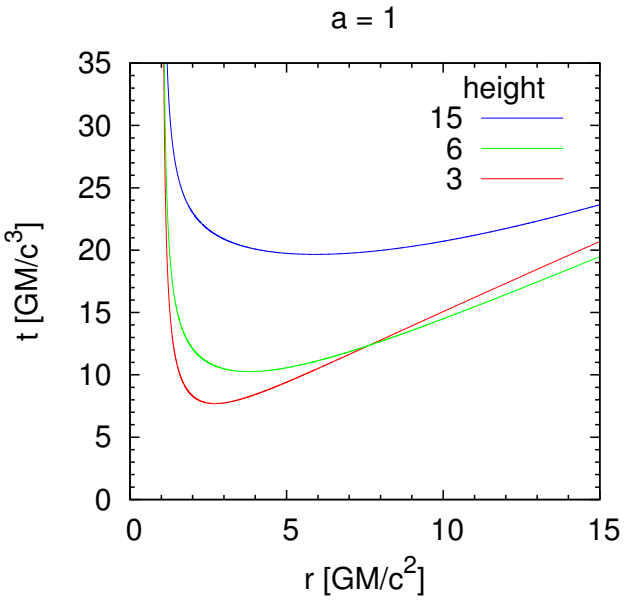


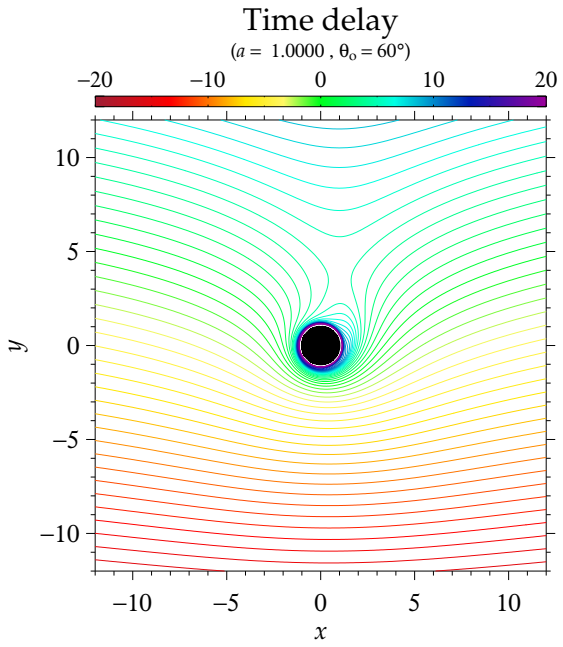


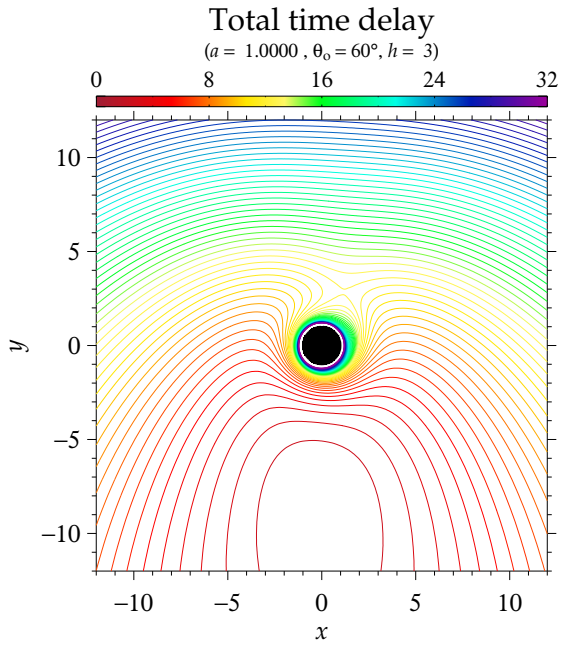


- total light travel time includes the lamp-to-disc and disc-to-observer part
- first photons arrive from the region in front of the black hole which is further out for higher source
- contours of the total time delay shows the ring of reflection that develops into two rings when the echo reaches the vicinity of the black hole

# Light curve

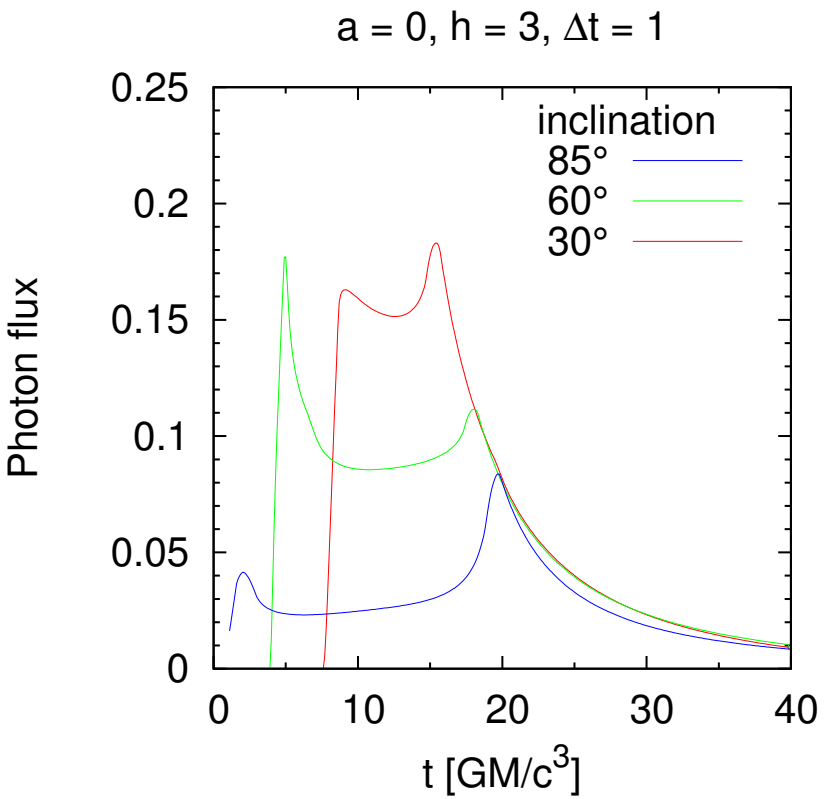


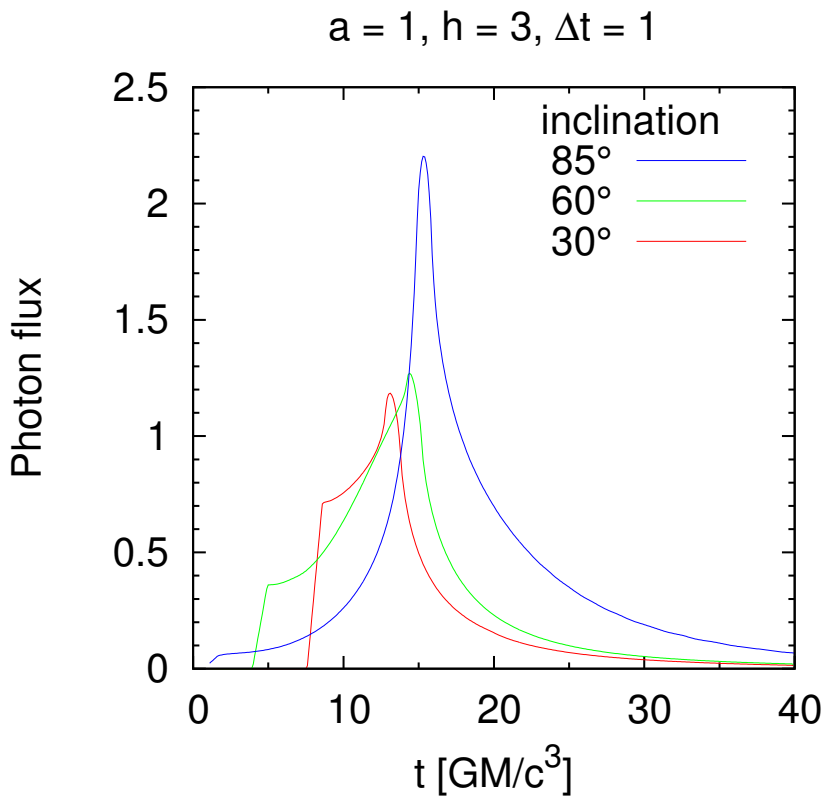


- the flux for Schwarzschild BH is much smaller than for Kerr BH due to the hole below ISCO (no inner ring in Schwarzschild case)
- the shape of the light curve differs substantially for different spins
- the “duration” of the echo is quite similar
- the higher the inclination the sooner first photons will be observed
- magnification due to lensing effect at high inclinations

# Dynamic spectrum – spectral line

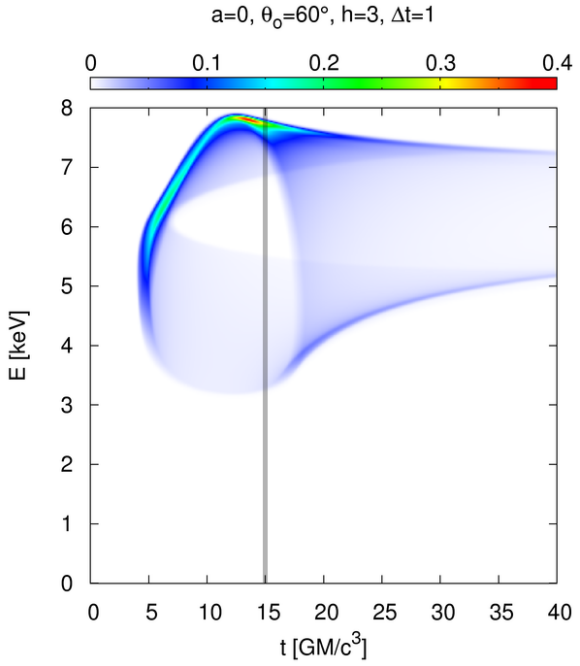


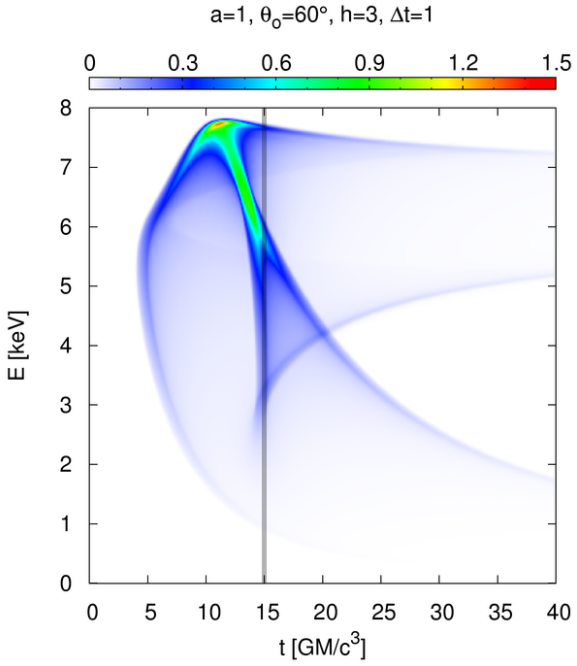


- signature of outer and inner echo in dynamic spectra
- large amplification when the two echos separate
- intrinsically narrow K$\alpha$ line can acquire weird shapes

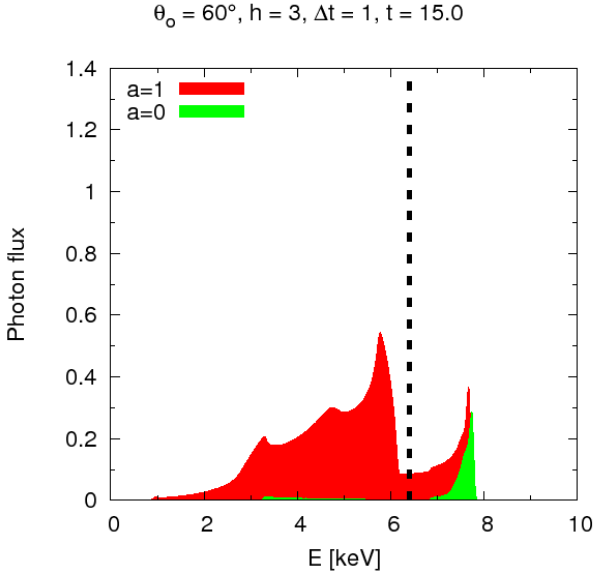

# Dynamic spectrum – ionised disc

$$E^2 \times F(E)$$

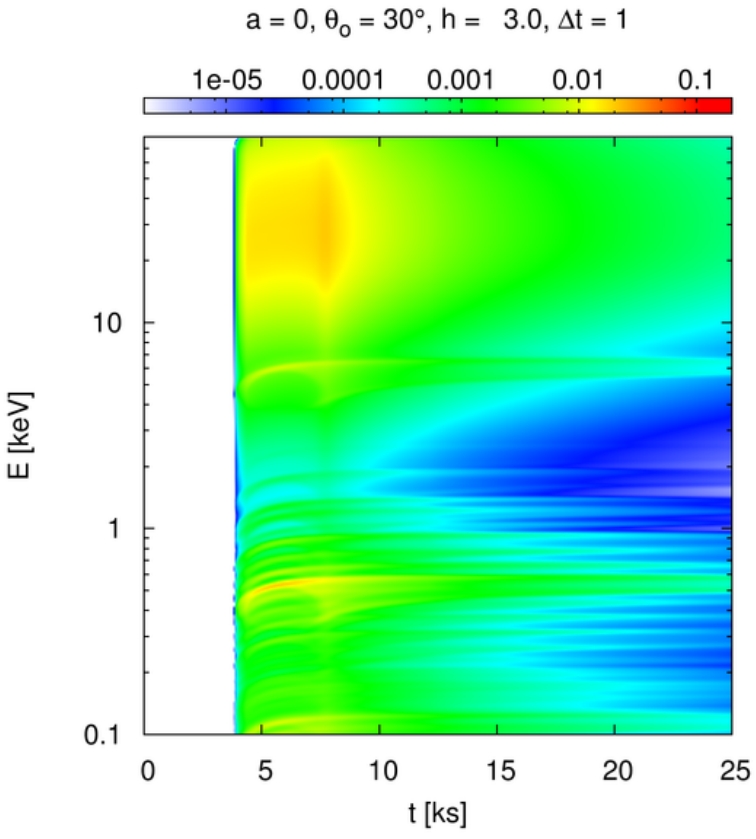


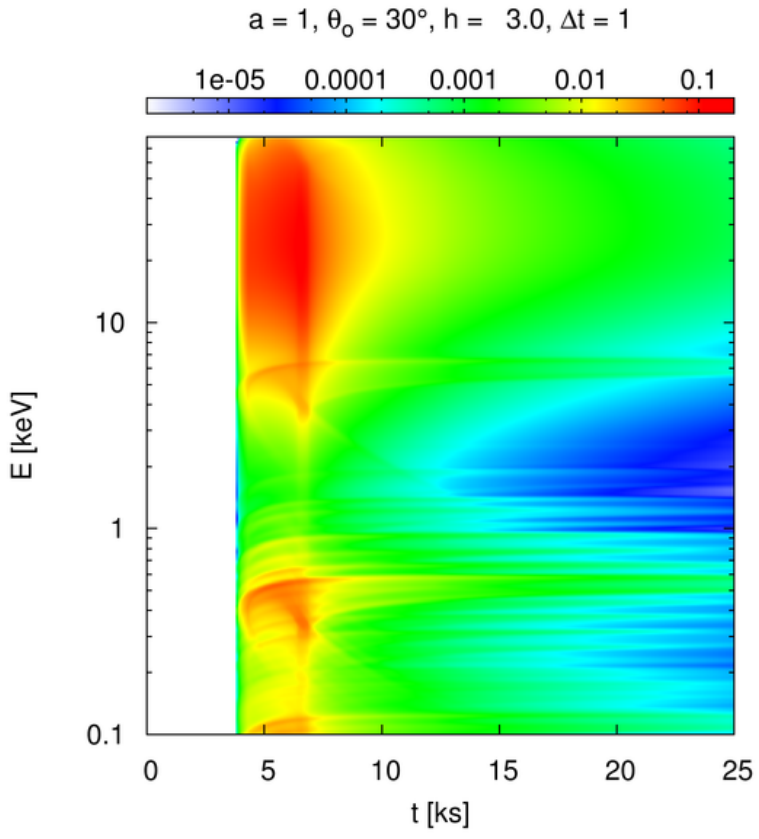

# Definition of the phase lag

$$F_{\mathrm{refl}}(E,t) = N_{\mathrm{p}}(t) * \psi(E,t) \qquad \Rightarrow \qquad \hat{F}_{\mathrm{refl}}(E,f) = \hat{N}_{\mathrm{p}}(f).\hat{\psi}(E,f)$$

where

$$\hat{\psi}(E,f) = A(E,f)e^{i\phi(E,f)}$$

---

if

$$N_{\mathrm{p}}(t) = \cos(2\pi f t) \qquad \text{and} \qquad \hat{\psi}(E) = A(E)e^{i\phi(E)}$$

then

$$F_{\mathrm{refl}}(E,t) = A(E)\cos\{2\pi f[t+\tau(E)]\} \qquad \text{where} \qquad \tau(E) \equiv \frac{\phi(E)}{2\pi f}$$

---

$$F(E,t) \sim N_{\mathrm{p}}(t) * (\psi_{\mathrm{r}}(E,t) + \delta(t)) \qquad \Rightarrow \qquad \hat{F}(E,f) \sim \hat{N}_{\mathrm{p}}(f).(\hat{\psi}_{\mathrm{r}}(E,f) + 1)$$

and

$$\tan\phi_{\mathrm{tot}}(E,f) = \frac{A_{\mathrm{r}}(E,f)\sin\phi_{\mathrm{r}}(E,f)}{1 + A_{\mathrm{r}}(E,f)\cos\phi_{\mathrm{r}}(E,f)}$$

# Parameter values and integrated spectrum

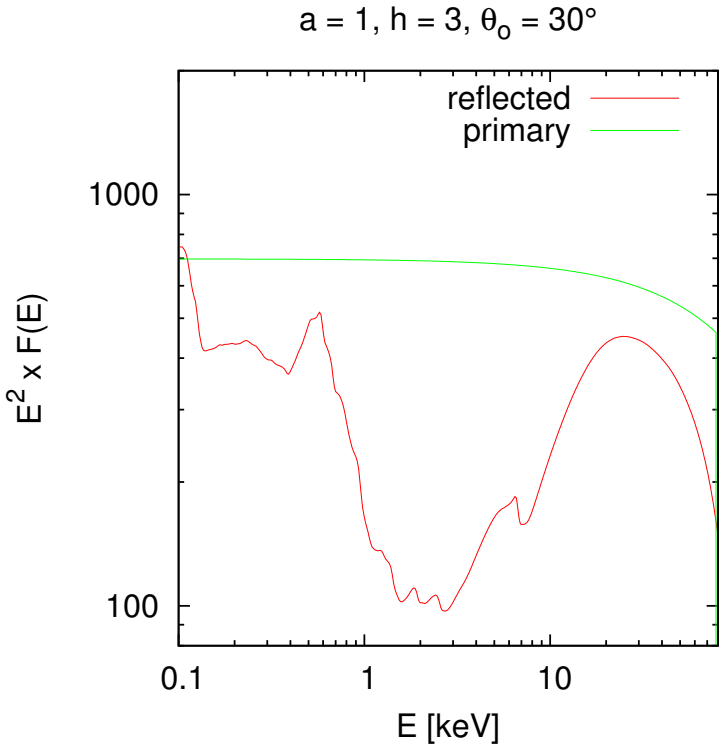


$$
\begin{aligned}
M &= 10^8 M_\odot \\
a &= 1\ (0) \\
\theta_o &= 30^\circ\ (60^\circ) \\
h &= 3\ (1.5,\ 6,\ 15,\ 30) \\
L_p &= 0.001\, L_{\mathrm{Edd}} \\
\Gamma &= 2\ (1.5,\ 3) \\
n_H &= 0.1\ (0.01,\ 50,\ 5,\ 0.2) \times 10^{15}\mathrm{cm}^{-3} \\
q_n &= -2\ (0,\ -5,\ -3)
\end{aligned}
$$

Energy bands: soft excess: $0.3 - 0.8$ keV

primary: $1 - 3$ keV

iron line: $3 - 9$ keV

Compton hump: $15 - 40$ keV

# Phase lag dependence on geometry

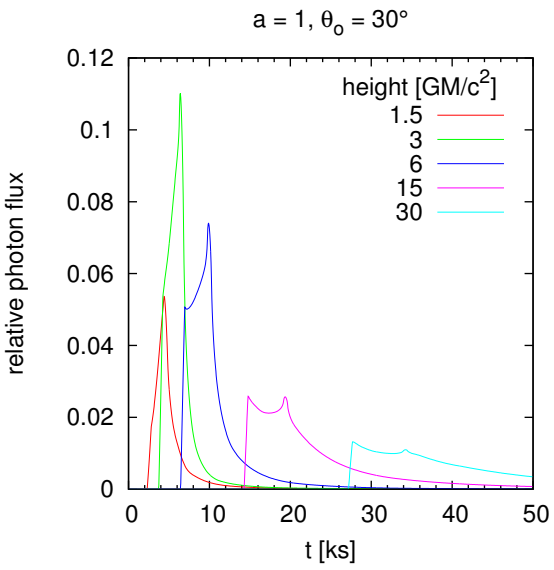


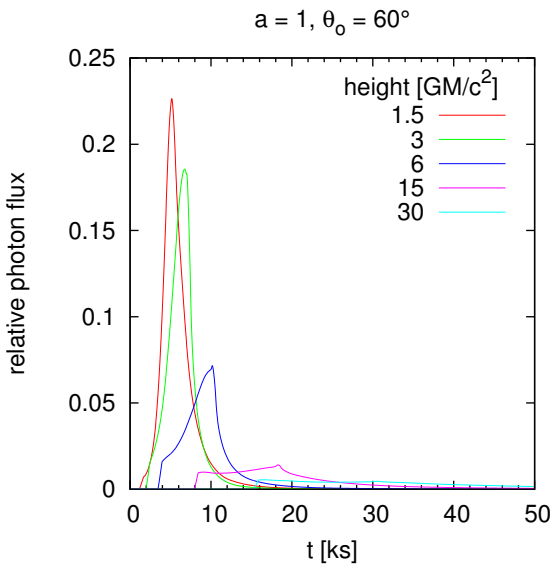


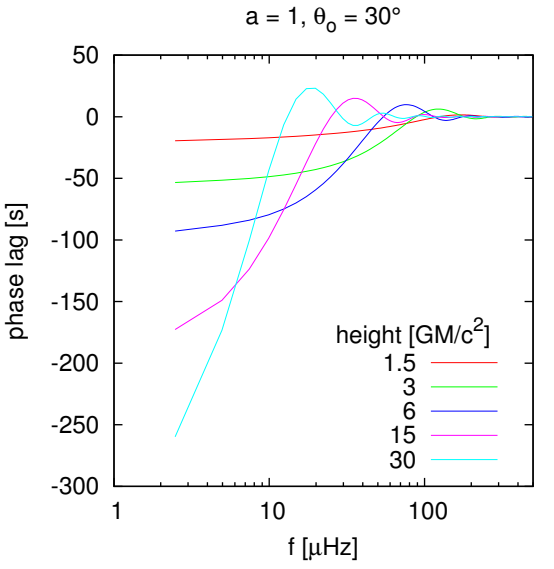


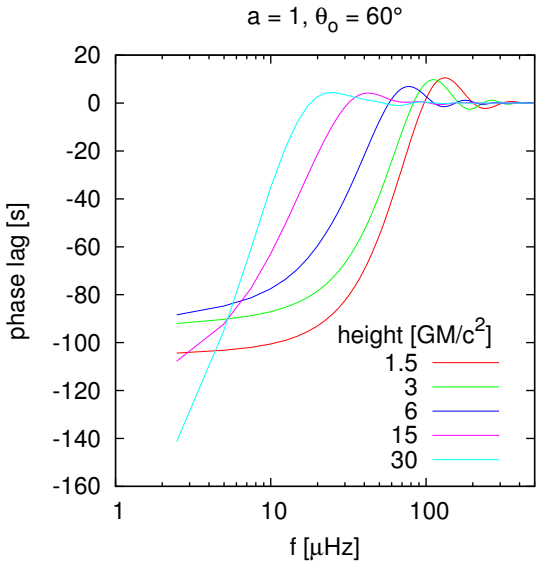


- reflected photon flux decreases with height
- primary flux increases with height
- the delay of response is increasing with height
- the “duration” of the response is longer
- the phase lag increases with height, it depends mainly on the “average” response time and magnitude of relative photon flux
- the phase lag null points are shifted to lower frequencies for higher heights due to longer timescales of response
- relative photon flux and the phase lag increase with inclination for low heights
- the delay and duration of response do not change much with the inclination and thus the phase lag null points frequencies change only slightly

# Phase lag dependence on spin and energy band

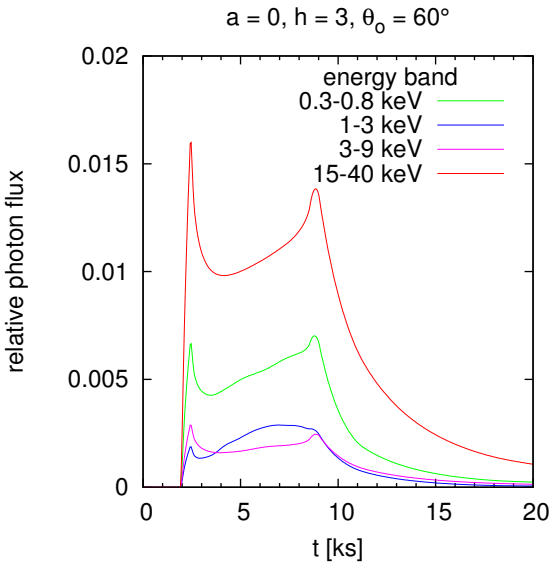


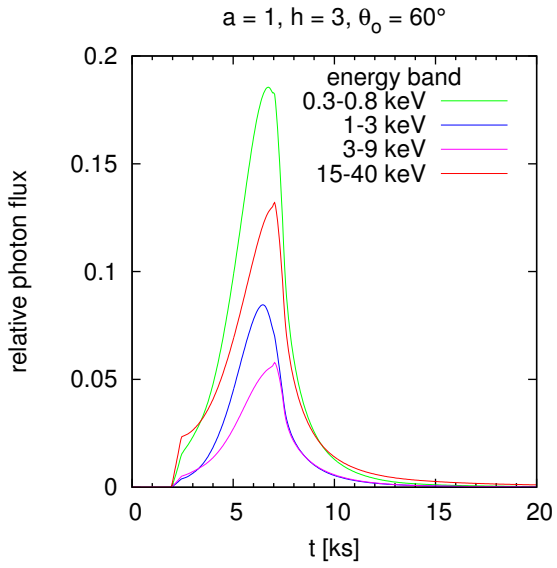


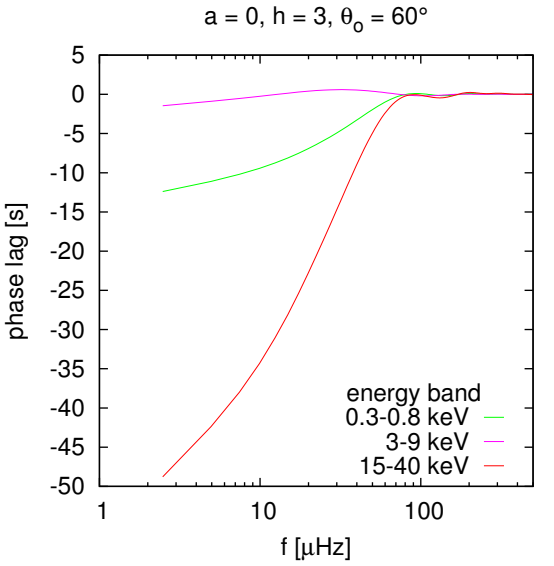


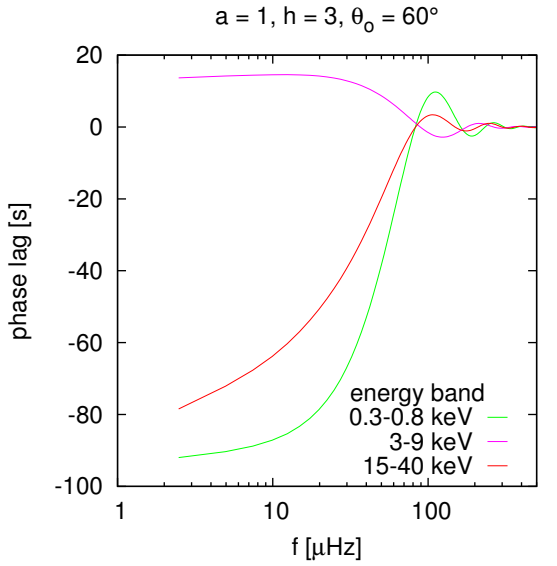


- the relative flux in the energy band where primary dominates may in some cases be larger than that in K$\alpha$ and Compton hump energy bands
- the magnitude of the phase lag in different energy bands differs (in extreme Kerr case the larger lag in SE is due to larger ionisation near BH)
- the magnitude of the phase lag is smaller in Schwarzschild case due to the hole in the disc under the ISCO
- the null points of the phase lag change only slightly with energy and spin

# Ionisation

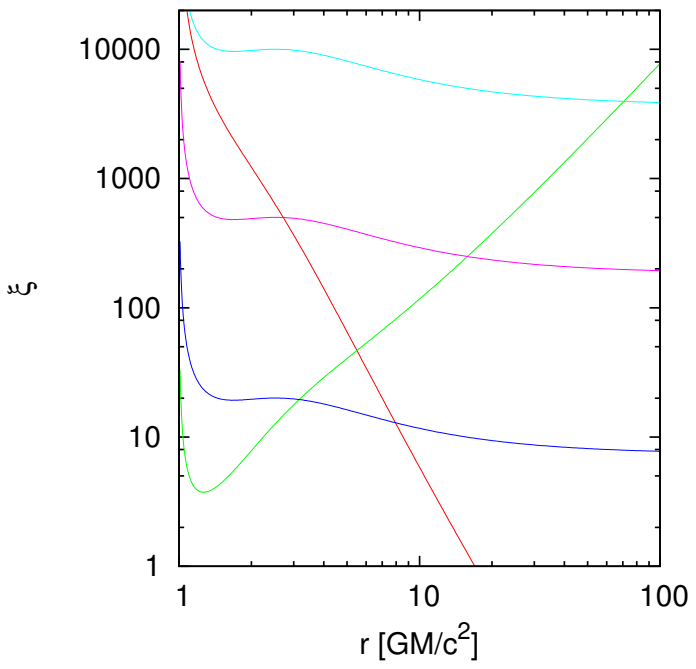


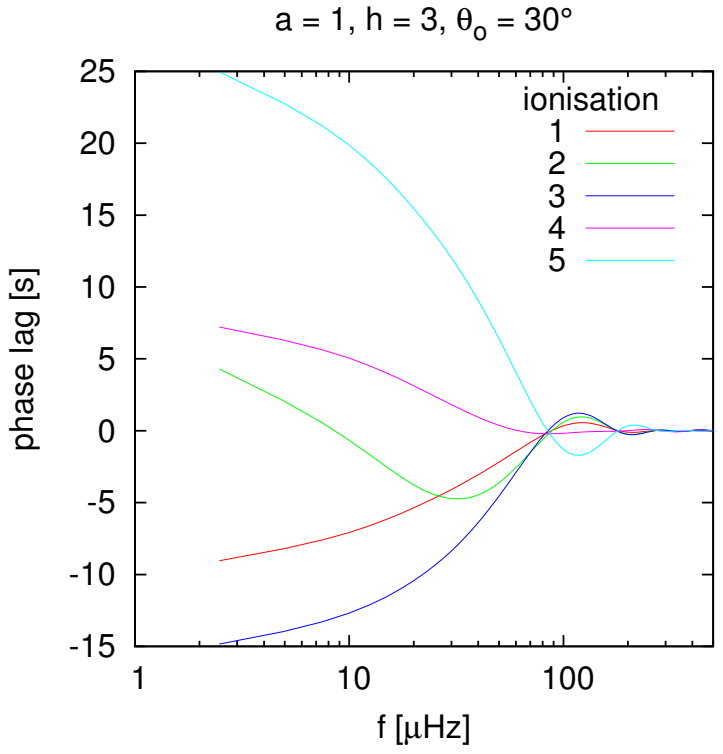


- the phase lag in K$\alpha$ band is shown
- the reflection component of the spectra are steeper for higher ionisation
- the magnitude of the phase lag depend on ionisation
- the null points of the phase lag does not change with the ionisation

# Directionality and photon index

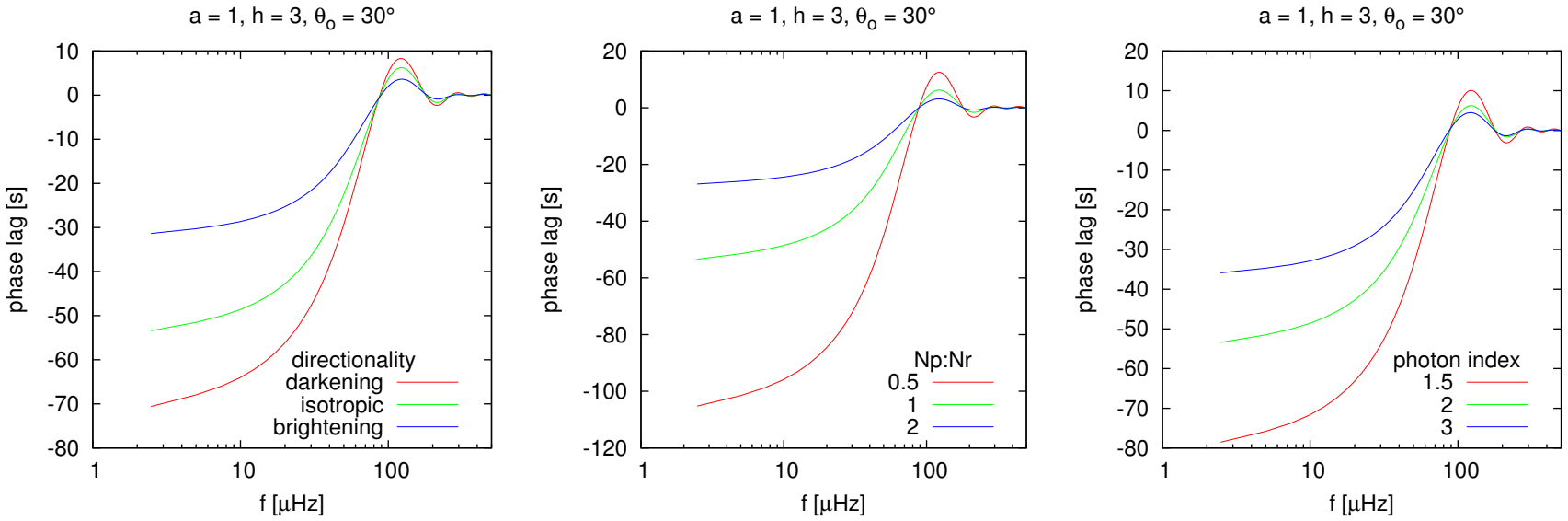


- the phase lag in SE band is shown
- the magnitude of the phase lag changes in all three cases
- the null points of the phase lag does not change with different directionility dependences or power-law photon index

# Phase lag energy dependence

for low $f$:

$$\begin{aligned} A_{\mathrm{r}}(E,f) &\simeq A_{\mathrm{E}}(E)A_{\mathrm{f}}(f) \\ \phi_{\mathrm{r}}(E,f) &\simeq \phi_{\mathrm{r}}(f) \end{aligned}$$

and

$$\Delta\tau(E,f) \simeq \frac{1}{2\pi f}\,\mathrm{atan}\,\frac{[A_{\mathrm{r}}(E,f)-A_{\mathrm{r}}(E_0,f)]\sin\phi_{\mathrm{r}}(f)}{1+[A_{\mathrm{r}}(E,f)+A_{\mathrm{r}}(E_0,f)]\cos\phi_{\mathrm{r}}(f)+A_{\mathrm{r}}(E,f)A_{\mathrm{r}}(E_0,f)}$$

and for $f$ such that $\phi_{\mathrm{r}}(f) = \pm\frac{\pi}{2}$:

$$\Delta\tau(E,f) \simeq \frac{1}{2\pi f}\,[A_{\mathrm{r}}(E,f)-A_{\mathrm{r}}(E_0,f)]$$

# Phase lag energy dependence

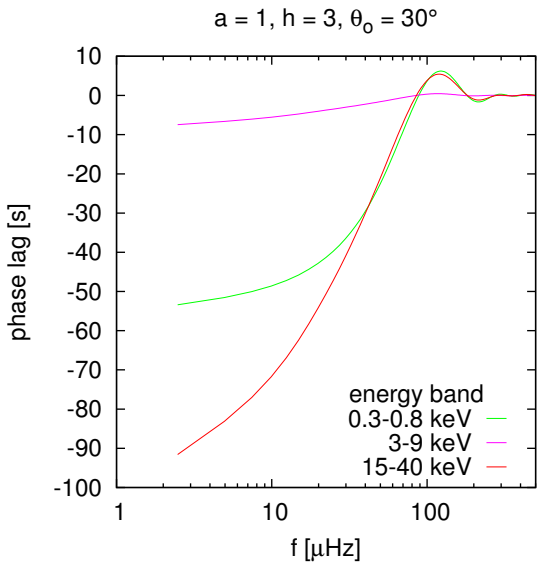


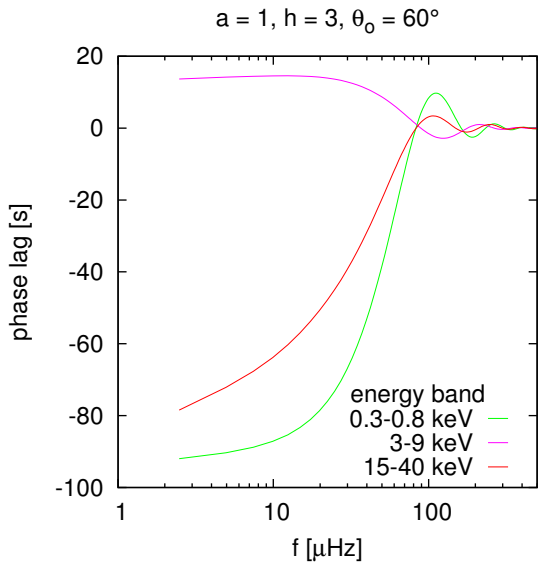


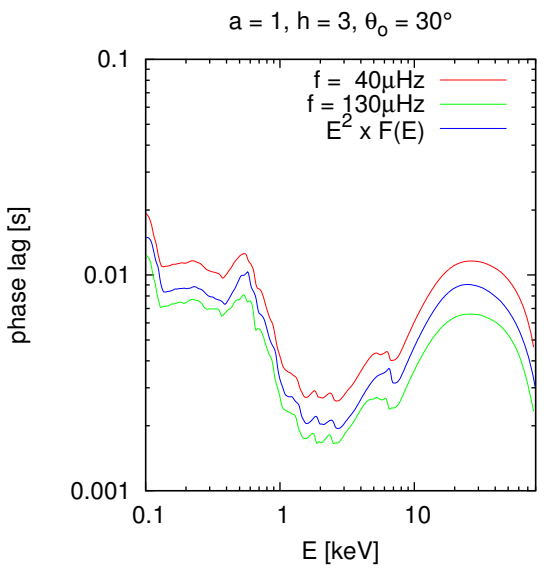


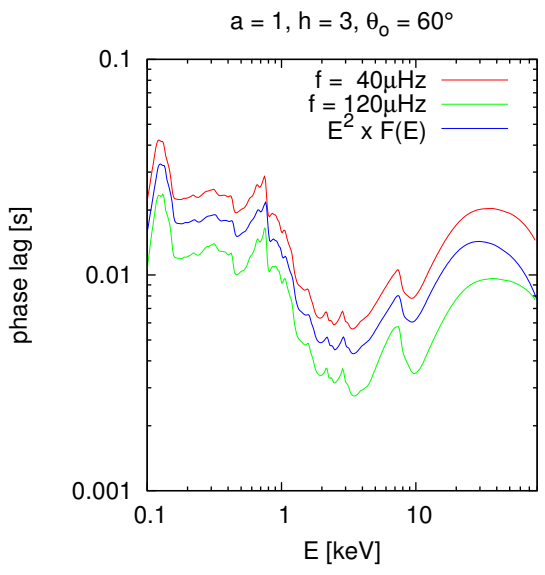


- the energy dependence of the phase lag follows the spectral shape perfectly at particular frequencies

# Phase lag energy dependence

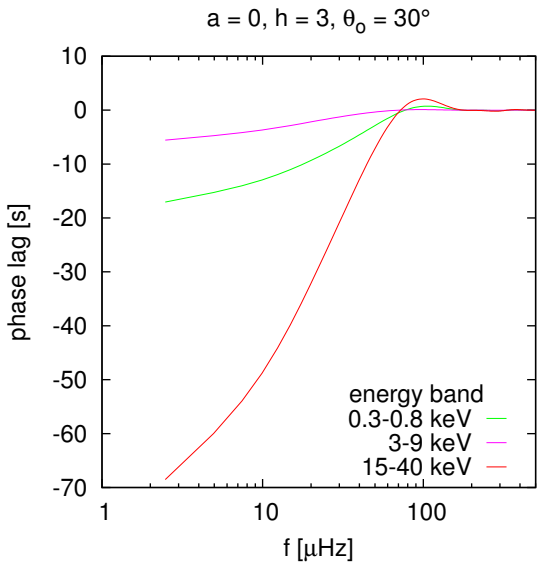


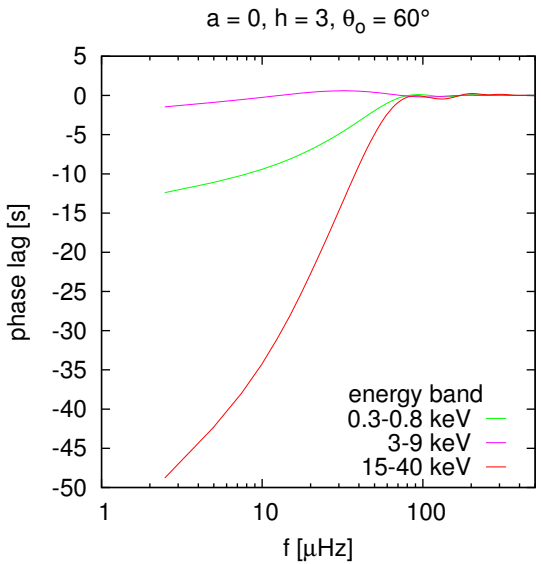


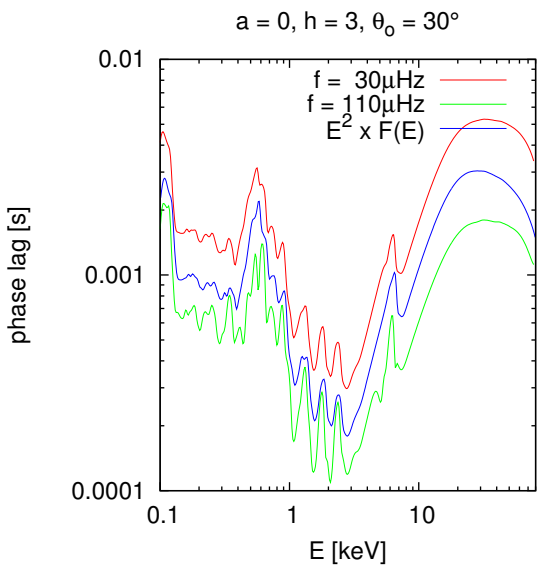


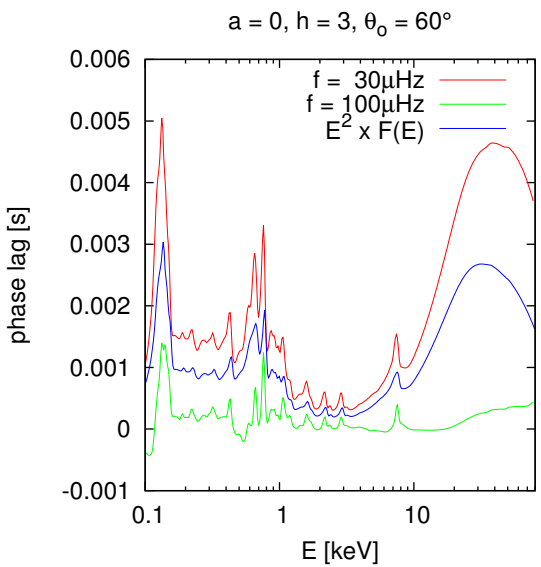


- if the second phase lag maximum is too small the phase lag energy dependence does not follow the spectral shape that well

# Summary

- the frequency dependence of the phase lag is mainly due to geometry (height of the corona)
- the magnitude of the phase lag depends on many details of the model (height, spin, ionisation, unisotropy, energy, ...)
- lag versus energy follows the spectral shape at the right frequencies
- extended corona

  $\rightarrow$ brings several new parameters

  (size, propagation speed, “ignition” position, inhomogeinities)

  $\rightarrow$ broadens the response of the disc